



## Radiation balance diversity on NW Spitsbergen in 2010–2014

Marek KEJNA<sup>1\*</sup>, Marion MATURILLI<sup>2</sup>, Andrzej ARAŻNY<sup>1</sup> and Ireneusz SOBOTA<sup>3</sup>

<sup>1</sup> Department of Meteorology and Climatology, Faculty of Earth Sciences,  
Nicolaus Copernicus University, Toruń, Lwowska 1, 87-100 Toruń, Poland  
<marek.kejna@umk.pl> <andy@umk.pl>

<sup>2</sup> Alfred Wegener Institute, Helmholtz Center for Polar and Marine Research,  
Telegrafenberg A43, 14473 Potsdam, Germany  
<marion.maturilli@awi.de>

<sup>3</sup> Department of Hydrology and Water Management, Faculty of Earth Sciences,  
Nicolaus Copernicus University, Toruń, Lwowska 1, 87-100 Toruń, Poland  
<irso@umk.pl>

\* corresponding author

**Abstract:** This article presents the results of observations of selected fluxes of the radiation balance in north-western Spitsbergen in the years from 2010 to 2014. Measurements were taken in Ny-Ålesund and in the area of Kaffiøyra, on different surface types occurring in the Polar zone: moraine, tundra, snow and ice. Substantial differences in the radiation balance among the various types of surface were observed. The observations carried out in the summer seasons of 2010–2014 in the area of Kaffiøyra demonstrated that the considerable reflection of solar radiation on the Waldemar Glacier (albedo 55%) resulted in a smaller solar energy net income. During the polar day, a diurnal course of the components of the radiation balance was apparently related to the solar elevation angle. When the sun was low over the horizon, the radiation balance became negative, especially on the glacier. Diurnal, annual and multi-annual variations in the radiation balance have a significant influence on the functioning of the environment in polar conditions.

Key words: Arctic, Svalbard, solar radiation, albedo, topoclimate.

### Introduction

Solar radiation is the main source of energy for numerous processes taking place on Earth. The solar radiation balance of the Earth's surface ( $Q^*$ ) determines the gains and losses of energy in the form of long- and shortwave radiation. It consists

of a shortwave radiation balance ( $K^*$ ) and a longwave radiation balance ( $L^*$ ), and is described by the following equations in the whole spectrum range (Oke 1987):

$$\begin{aligned} Q^* &= K^* + L^*; \\ K^* &= K\downarrow - K\uparrow; \\ L^* &= L\downarrow - L\uparrow; \\ Q^* &= (K\downarrow - K\uparrow) + (L\downarrow - L\uparrow) \end{aligned}$$

where:

$Q^*$  – net radiation balance,

$K^*$  – net shortwave solar radiation,

$L^*$  – net longwave solar radiation,

$K\downarrow$  – incoming shortwave solar radiation (direct and diffuse),

$K\uparrow$  – outgoing shortwave solar radiation, reflected by the active surface,

$L\downarrow$  – incoming longwave radiation,

$L\uparrow$  – outgoing longwave radiation, emitted by the active surface.

In polar regions there are specific lighting and climate conditions (Przybylak 2016). The all-day solar radiation during the polar day, or its total lack during the polar night affect the state and functions of the environment.

There are a number of positive feedback mechanisms in the Arctic, enhancing global warming, the so-called ‘Arctic amplification’ (Serreze and Barry 2011). In the area of Svalbard the annual mean temperature of air in the period 1892 to 2012 increased by 2.6°C/100 years (Nordli *et al.* 2014). One of the amplification mechanisms is the snow/ice-albedo feedback which affects the radiation and heat balance of the Arctic Ocean by reduction of the sea ice cover (Screen and Simmonds 2010; Iskasen *et al.* 2016). Quicker melting snow cover on the land also favours absorption of solar radiation due to a decreased albedo (Maturilli *et al.* 2015). Ablation increases and a negative glacier mass balance is manifested by retreating glacier fronts and an overall deglaciation of the area. On Svalbard, the glaciated area has decreased by an average of 80 km<sup>2</sup> over the past 30 years, representing a reduction of 7% (Nuth *et al.* 2013) and about 42% in the Kaffiøyra region (Sobota 2013). The permafrost is also degrading (Etzelmüller *et al.* 2011), including the one in NW Spitsbergen (Sobota and Nowak 2014; Arażny *et al.* 2016).

Higher air temperature in the Arctic is also connected with an increased interzone air circulation which brings in warmer air masses with an extra water vapour content (Curry *et al.* 1996; Isaksen *et al.* 2016). At the same time, the sky is more covered with clouds in all seasons of the year (Eastman and Warren 2010). The increase in cloud amount affects the radiation balance, both negatively (shortwave radiation) and positively (longwave radiation), which results in a global augmentation of heat resource in the polar environment

(Nardino and Georgiadis 2003; Shupe and Intieri 2004; Zygmunowska *et al.* 2012). The measurements of radiation balance conducted at Ny-Ålesund (NW Spitsbergen, 78.92°N, 11.92°E) in 1992–2013 as a part of the Baseline Surface Radiation Network (BSRN) revealed its increase by  $4.9 \pm 2.9 \text{ W m}^{-2}$  per decade. In particular, the longwave downward atmospheric radiation increased in the winter season by  $15.6 \text{ W m}^{-2}$  per decade, and a smaller increase was noted in the case of shortwave radiation in the summer season ( $+4.9 \text{ W m}^{-2}/\text{decade}$ ) (Maturilli *et al.* 2015).

On Spitsbergen, measurements of solar radiation and radiation balance components have been carried out in several areas. Near the Polish Polar Station at Hornsund, for example, observations were started by Kosiba (1960) and were later continued on multiple occasions (Głowicki 1985; Prošek and Brázdil 1994; Styszyńska 1997; Marsz and Styszyńska 2007; Budzik *et al.* 2009). Since 1974, an actinometric station has been in operation at Ny-Ålesund by the Norwegian Polar Institute and relevant results of the observations can be found in the following publications: Vinje (1974–82); Hisdal (1986); Hisdal *et al.* (1992); Ørbaek *et al.* (1999); Budzik (2004). From 1992, the Alfred Wegener Institute operates surface radiation measurements in Ny-Ålesund contributing to BSRN (Kupfer *et al.* 2006; Maturilli *et al.* 2015). Regular observations of the radiation and heat balance have also been carried out at the nearby Kongsvegen Glacier and the results for 2001–2010 can be found in an article by Karner *et al.* (2013). In the area of Kaffiøyra, actinometric measurements have been performed since 1978 (Wójcik 1989; Wójcik and Marciniak 1993, 2002; Kejna 2000; Caputa *et al.* 2002; Budzik 2003; Kejna *et al.* 2011, 2012 and others). Topoclimatic studies of solar radiation and radiation balance have also been conducted on Spitsbergen, demonstrating a considerable diversity of the radiation balance, depending on the type of surface (albedo) and exposure of the terrain (Gluza and Siwek 2005; Arnold and Rees 2009; Budzik *et al.* 2009; Kryza *et al.* 2010; Kejna *et al.* 2011, 2012).

Here, we analyse the spatial diversity of the radiation balance components in the north-west part of Spitsbergen in an annual course on the basis of data from 2013–2014 and in a diurnal course on the basis of summer season data from 2010–2014. The spatial diversity of energy absorbed by the ground will provide more insight into the understanding of the way the climate system functions in a polar environment.

## Research area

The observations were carried out in two relatively near areas of NW Spitsbergen: Ny-Ålesund (NYA) and the area of the Nicolaus Copernicus University Polar Station at Kaffiøyra-Heggodden (KH), that have a distance of approx. 30 km. The measurement data for Ny-Ålesund were sourced from

the AWIPEV Research Base, whereas for Kaffiøyra data derived from the Department of Meteorology and Climatology and NCU Polar Station of the Nicolaus Copernicus University in Toruń (Poland).

In this analysis, the total solar radiation at NYA and KH was compared for the period from August 2013 to August 2014, as well as the individual radiation balance fluxes in the summer seasons of 2010–2014 (21 July–31 August). The measurements of radiation balance are conducted on tundra. In the area of Kaffiøyra, the radiation balance was additionally measured on other typical Arctic surfaces: the moraines of the Aavatsmark Glacier (KH) and of the Waldemar Glacier (LW1), in the tundra (KT) and on snow- and ice-covered surfaces of the Waldemar Glacier's firn field (LW2). The basic information concerning the measurement sites is provided in Table 1 and their locations in Figure 1.

The locations of the measurement sites were not substantially different from the astronomical point of view. The polar day at NYA lasts from 18 April to 24 August, and the polar night begins on 24 October and ends on 18 February. On the KH, polar day and polar night are 1 day shorter, respectively. However, the orography of the nearby landforms, limiting the amount of incoming direct solar radiation, is an important diversifying factor. At NYA, because of the shadows from the nearby Zeppelin Mountains, the rays of sunlight reach the measurement site between 8 March and 8 October (Maturilli *et al.* 2015).

Table 1

Location of meteorological sites in NW Spitsbergen from which data were used.

| Symbol | Site                        | Latitude | Longitude | altitude | Surface      | Summer seasons |
|--------|-----------------------------|----------|-----------|----------|--------------|----------------|
| NYA    | Ny-Ålesund                  | 78°56' N | 11°57' E  | 8        | Tundra       | 2010–2014      |
| KH     | Kaffiøyra-Heggodden         | 78°41' N | 11°50' E  | 11       | Moraine      | 2010–2014      |
| KT     | Tundra                      | 78°40' N | 11°52' E  | 90       | Tundra       | 2011–2012      |
| LW1    | Waldemar Glacier-front      | 78°41' N | 12°00' E  | 130      | Moraine      | 2010           |
| LW2    | Waldemar Glacier-firn field | 78°41' N | 12°05' E  | 375      | Snow and ice | 2010–2014      |

In the area of Kaffiøyra (KH and KT), the horizon of the measurement site is more favourable as any higher terrain obstacles are only situated in the north and east, therefore the sun is obstructed in its lower culmination, in particular at the end of the polar day. Substantial orographic limitations occur at the front (LW1) and the firn field (LW2) of the Waldemar Glacier, surrounded by mountains from three sides and free from obstacles only in the south west, along the glacial tongue (Kejna 2012).

Despite the short distance, considerably different weather conditions may occur in the two compared areas. The climatological situation of NYA has

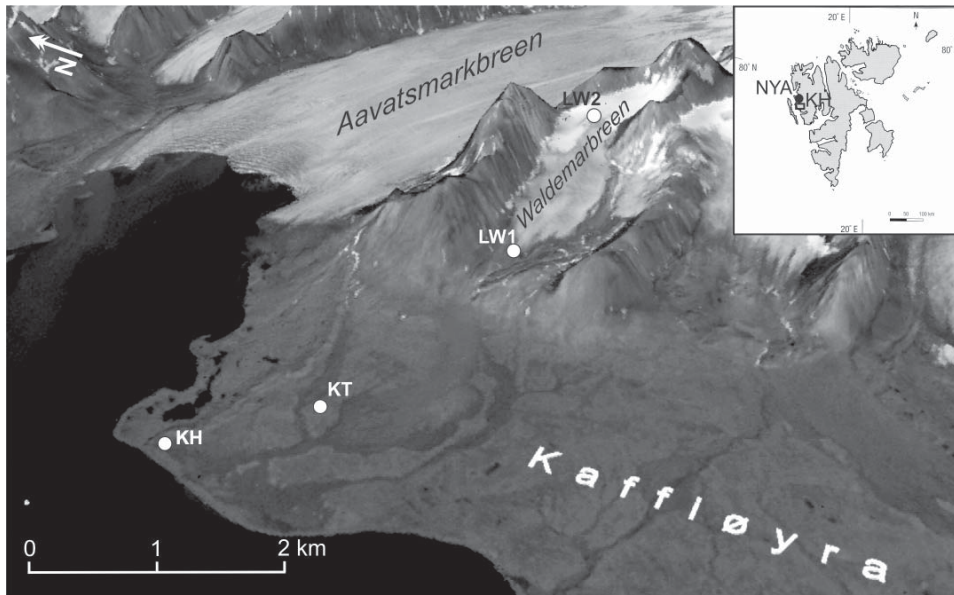


Fig. 1. Location of meteorological sites in NW Spitsbergen from which data were used in the study.

been described by Maturilli *et al.* (2014). The cloudiness in the area of NYA is lesser than at Hornsund (SW Spitsbergen); in 1975–2000 the average degree of cloudiness was 6.6 and 7.2, respectively, on a scale of 0–8 (82–90%). It is an effect of the local orography and katabatic winds reaching the NYA site. In summer, at NYA is less cloudy than at KH, reaching 79% and 84%, respectively (Przybylak and Arażny 2006). At KH, clouds of the *Stratus* are formed and move along the Forlandsundet (Przybylak *et al.* 2012). On the Waldemar Glacier, on the other hand, the degree of cloudiness is higher but sometimes sunny spells occur, typical of glacial areas and the interior of Spitsbergen, *e.g.* on the Kongsvegen Glacier (Kupfer *et al.* 2006).

## Methods

The Ny-Ålesund data were retrieved from measurements with pyranometers (Kipp&Zonen CM11 and CMP22) for diffuse radiation, a pyrliometer (Eppley NIP) for direct radiation, and pyrgeometers (Eppley PIR) for longwave radiation (Maturilli *et al.* 2015).

In the area of Kaffiøyra, registration of all components of the solar radiation balance was started using Kipp&Zonen CNR4 net radiometers in the summer of 2010 (Kejna *et al.* 2011) – Fig. 2. In August 2013, an automatic weather

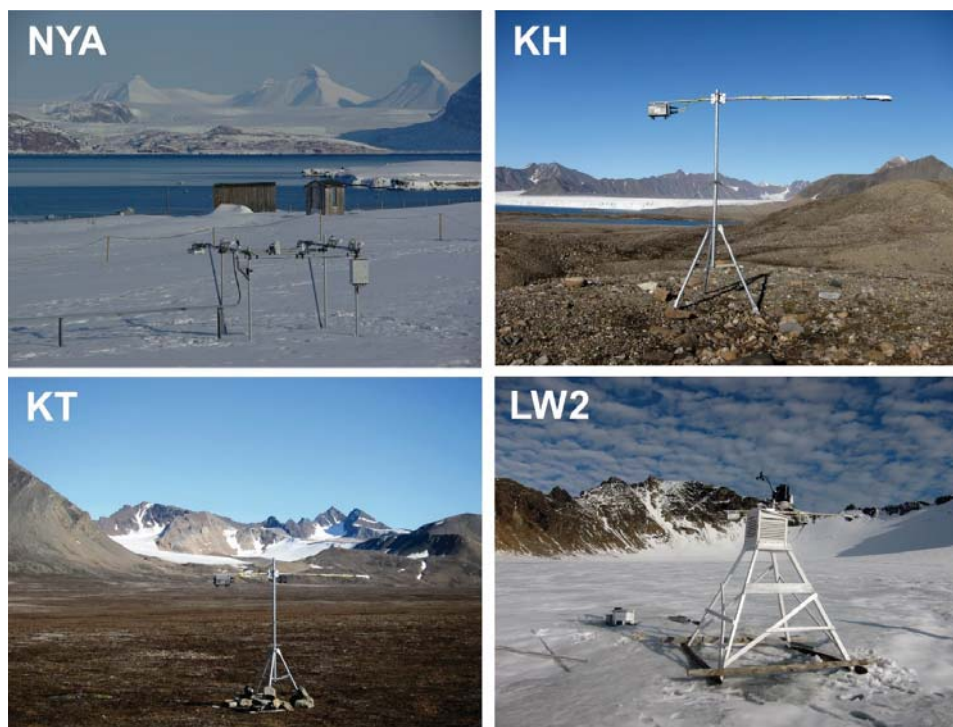


Fig. 2. Measurement stands in Ny-Ålesund (photo Jürgen Graeser) and in the Kaffiøyra region (photo M. Kejna). Explanation of symbol in Table 1.

station, equipped with a HOBO Silicon Pyranometer Smart Sensor was installed at KH to record solar radiation data all year round.

The sensors at all sites were placed about 2 m above ground level. The sites were selected to represent the typical surfaces in that area: moraine, tundra and glacier. The instruments were inspected and cleaned on regular basis. At the KH site, during the automatic observations carried out all year round (HOBO automatic weather station), there was no supervision, however the design of the equipment and the prevailing high winds prevented accumulation of snow. The measurements were taken using the local time zone.

## Results and interpretation

**Annual course of radiation balance.** — The incoming solar radiation  $K_{\downarrow}$  is determined by astronomical factors connected with variable declination of the sun, geographical location of the area (latitude), local obscuring of the horizon and exposure, as well as by atmospheric factors: cloudiness and water vapour

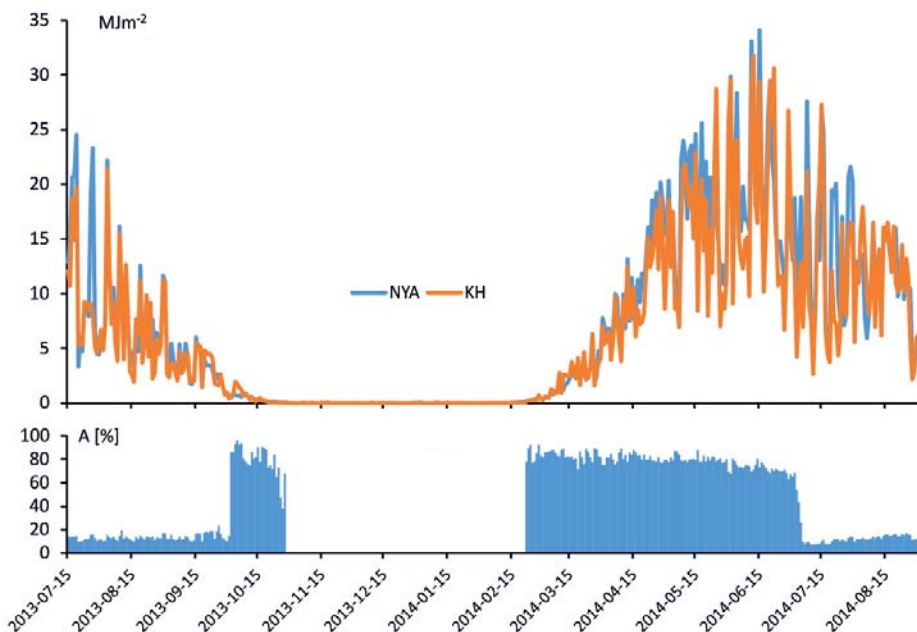


Fig. 3. Course of solar global radiation at Ny-Ålesund (NYA) and Kaffiøyra (KH; upper graph) and albedo (NYA; lower graph) in the period 15 July 2013 to 31 August 2014.

and aerosol content in the atmosphere. Solar radiation reaches the ground in a direct or diffuse form. In Arctic conditions, with ample cloudiness, the share of direct radiation is small and diffuse radiation prevails (Hisdal 1986).

Parallel observations carried out at NYA and KH from 15 July 2013 to 31 August 2014 revealed a substantially comparable course of  $K_{\downarrow}$  (Fig. 3). The Pearson linear correlation coefficient was 0.95.

An average rate of  $K_{\downarrow}$  at NYA reached  $73.6 \text{ Wm}^{-2}$ , and sum of  $K_{\downarrow}$  was determined at  $2322.6 \text{ MJ m}^{-2}$ , on the basis of an annual series of observations (August 2013 – July 2014), whereas at the same time at KH the recorded solar radiation was  $66.3 \text{ Wm}^{-2}$  ( $2089.4 \text{ MJ m}^{-2}$ ) – Table 2.

The highest  $K_{\downarrow}$  occurred in June 2014 at the NYA  $239.5 \text{ Wm}^{-2}$  ( $597.4 \text{ MJ m}^{-2}$ ) and at the KH  $216.9 \text{ Wm}^{-2}$  ( $560.0 \text{ MJ m}^{-2}$ ), when diurnal sums exceeded  $30 \text{ MJ m}^{-2}$  (NYA:  $34.1 \text{ MJ m}^{-2}$  and KH:  $31.8 \text{ MJ m}^{-2}$ ). Higher  $K_{\downarrow}$  in most months were observed at the NYA site, situated further to the north. This is due to a smaller cloudiness amount at the NYA (Przybylak and Araźny 2006).

Most of the solar radiation is reflected from the surface ( $K_{\uparrow}$ ), particularly in spring when the snow cover still persists. For example, in May 2013 at NYA  $159.5 \text{ Wm}^{-2}$  ( $427.9 \text{ MJ m}^{-2}$ ) was reflected, and the albedo reached 79.6%. When the snow melted, the albedo dropped to 13–17% (Fig. 3). The shortwave

radiation balance ( $K^*$ ) at NYA was  $32.1 \text{ Wm}^{-2}$  ( $1011.8 \text{ MJ m}^{-2}$ ), 65% of which fell on July and August (*e.g.* in 2014 it was  $362.3 \text{ MJ m}^{-2}$  and  $296.2 \text{ MJ m}^{-2}$ , respectively).

Table 2

Monthly values of radiation balance fluxes at Ny-Ålesund (NYA) and global solar radiation at Kaffiøyra (KH) in  $\text{MJ m}^{-2}$  in the period July 2013 to August 2014 (– represents no data).

| Month                 | K↓     |        | K↑     | A (%) | L↑     | L↓     | K*     | L*      | Q*     |
|-----------------------|--------|--------|--------|-------|--------|--------|--------|---------|--------|
|                       | NYA    | KH     | NYA    | NYA   | NYA    | NYA    | NYA    | NYA     | NYA    |
| Jul 2013              | 388.0  | .      | 49.6   | 13.1  | 921.6  | 816.4  | 338.4  | -105.1  | 233.2  |
| Aug 2013              | 244.3  | 228.9  | 32.8   | 13.8  | 915.8  | 830.4  | 211.5  | -85.4   | 126.1  |
| Sep 2013              | 94.4   | 92.7   | 13.2   | 14.8  | 841.1  | 755.2  | 81.1   | -85.9   | -4.8   |
| Oct 2013              | 9.6    | 13.5   | 7.7    | –     | 735.1  | 642.9  | 1.9    | -92.3   | -90.4  |
| Nov 2013              | –      | –      | –      | –     | 680.1  | 599.6  | –      | -80.4   | -80.4  |
| Dec 2013              | –      | –      | –      | –     | 699.2  | 587.6  | –      | -111.6  | -111.6 |
| Jan 2014              | –      | –      | –      | –     | 752.5  | 688.4  | –      | -64.1   | -64.1  |
| Feb 2014              | 2.2    | 2.4    | 1.7    | –     | 696.2  | 631.8  | 0.5    | -64.4   | -63.9  |
| Mar 2014              | 69.8   | 75.5   | 56.6   | 81.5  | 695.7  | 606.1  | 13.2   | -89.6   | -76.4  |
| Apr 2014              | 332.7  | 289.1  | 267.8  | 80.6  | 666.8  | 560.6  | 64.9   | -106.1  | -41.2  |
| May 2014              | 537.7  | 484.8  | 427.9  | 79.6  | 783.8  | 702.3  | 109.8  | -81.5   | 28.3   |
| Jun 2014              | 597.4  | 560.0  | 430.9  | 72.1  | 811.3  | 747.4  | 166.4  | -63.9   | 102.5  |
| Jul 2014              | 434.6  | 342.6  | 72.2   | 16.8  | 927.7  | 837.9  | 362.3  | -89.8   | 272.5  |
| Aug 2014              | 344.3  | 348.3  | 48.1   | 14.1  | 923.3  | 778.1  | 296.2  | -145.2  | 151.1  |
| Aug 2013<br>–Jul 2014 | 2322.6 | 2089.4 | 1310.9 | 56.4  | 9205.2 | 8190.0 | 1011.8 | -1015.2 | -3.4   |

Explanation of symbols – see text on page 62.

The ground surface becomes a source of longwave terrestrial radiation  $L\uparrow$ , which at NYA amounted to  $291.9 \text{ Wm}^{-2}$  ( $9205.2 \text{ MJ m}^{-2}$ ). The highest  $L\uparrow$  was observed, in July 2014 ( $346.4 \text{ Wm}^{-2}$ ,  $927.7 \text{ MJ m}^{-2}$ ) which is the time when the surface ground temperature was the highest. In the cold half of the year,  $L\uparrow$  was markedly lower ( $257.3 \text{ Wm}^{-2}$ ,  $666.8 \text{ MJ m}^{-2}$  in April 2014). This kind of radiation largely returns from the atmosphere, which becomes an important source of energy for the surface. In the analysed year, the overall amount of  $L\downarrow$  at NYA was  $259.7 \text{ Wm}^{-2}$  ( $8190.0 \text{ MJ m}^{-2}$ ). The longwave radiation balance ( $L^*$ ) at NYA was negative,  $-32.2 \text{ Wm}^{-2}$  ( $-1015.2 \text{ MJ m}^{-2}$ ).

In 2014, the radiation balance ( $Q^*$ ) at NYA was found to be negative  $-0.11 \text{ Wm}^{-2}$  ( $-3.4 \text{ MJ m}^{-2}$ ), however some energy surplus was observed from May to August that year, *e.g.* in July  $101.7 \text{ Wm}^{-2}$  ( $272.5 \text{ MJ m}^{-2}$ ). In all the other months energy losses prevail.



### Dependence of radiation balance fluxes on atmospheric factors. —

The optical state of atmosphere (aerosol, clouds and water vapour content) has a substantial influence on individual components of  $Q^*$ . The transmittance characteristics of the atmosphere were determined by comparing measured values of  $K_{\downarrow}$  with the calculated radiation sum at the top of the atmosphere  $K_{TOA}$ .

Potential irradiance changes with the declination of the sun, which affects the sun's apparent position over the horizon and the length of the day. The amount of solar radiation at the upper boundary of the atmosphere on the NW Spitsbergen was determined using the following formula (Hartmann 1994):

$$K_{TOA} = \frac{E_0 I_{SC} \cdot \zeta}{\pi} (h_0 \sin \varphi \sin \delta + \cos \varphi \cos \delta \sin h_0)$$

where:

$K_{TOA}$  – diurnal sum of radiant energy reaching a horizontal surface at the top of atmosphere ( $\text{MJm}^{-2}$ ).

$E_0 I_{SC}$  – solar constant calculated for each day of the year ( $I_{SC}=1367 \text{ Wm}^{-2}$ ).

$\zeta$  – number of seconds in 24 hours (86 400).

$h_0$  – solar hour angle (rad).

$\varphi$  – latitude at the point of observation (rad).

$\delta$  – declination of the sun on a given day (rad).

A detailed methodology has been described by Kejna *et al.* (2014).

As much as  $4739.7 \text{ MJ m}^{-2}$  of solar energy reached the upper limit of the atmosphere at NYA, and the annual sum of  $K_{\downarrow}$  was  $2322.6 \text{ MJ m}^{-2}$  (Table 3). Hence, the annual average transmittance of  $K_{\downarrow}$  was determined at 49.0%. During the year, the months of the greatest transmittance were April (57.7%). This indicates a smaller degree of cloudiness and a greater atmospheric transparency. In April the mean cloudiness at NYA was only 5.7 (in the 0–8 scale) in the period 1975–2000 (Przybylak and Arażny 2010). At KH, out of the total sum of radiation,  $4807.3 \text{ MJ m}^{-2}$  at the upper limit of the atmosphere, only 43.5% of solar energy reached the ground. May and June were the only two months of 2014 when the transmittance of  $K_{\downarrow}$  exceeded 50%.

The influence of individual meteorological elements on the fluxes of  $Q^*$  were analysed for the KH station taking into account diurnal values of cloudiness, sunshine duration and relative humidity of the air from 21 July to 31 August of the years 2010–2014 (210 days altogether). Substantial correlations of the fluxes of  $Q^*$  with selected meteorological elements were found on the basis of a linear correlation analysis (Table 4).

Increased cloudiness had a significant influence on a drop in  $K_{\downarrow}$  and  $K_{\uparrow}$  (Pearson linear correlation coefficient,  $r = -0.71$ ). When the sky is cloudy (overcast), only diffuse radiation reaches the ground. The  $K^*$  revealed a similar

Table 3

Monthly sums of global solar radiation ( $K\downarrow$ ) at the top of atmosphere and at Ny-Ålesund (NYA) and Kaffiøyra (KH) in  $\text{MJ m}^{-2}$  in the period July 2013 to August 2014.

| Month                 | $K\downarrow$ at the top of atmosphere ( $\text{MJ m}^{-2}$ ) |        | $K\downarrow$ at the surface ( $\text{MJ m}^{-2}$ ) |        | Transmittance $K\downarrow$ (%) |      |
|-----------------------|---|--------|---|--------|---------------------------------|------|
|                       | NYA   | KH     | NYA   | KH     | NYA                             | KH   |
| Jul 2013              | 979.1   | 993.5  | 388.0   |        | 39.6                            |      |
| Aug 2013              | 736.7   | 745.6  | 244.3   | 228.9  | 33.2                            | 30.7 |
| Sep 2013              | 311.2   | 314.9  | 94.4  | 92.7   | 30.3                            | 29.4 |
| Oct 2013              | 36.6  | 38.8   | 9.6   | 13.5   | 26.2                            | 34.7 |
| Nov 2013              | –   | –      | –   | –      | –                               | –    |
| Dec 2013              | –   | –      | –   | –      | –                               | –    |
| Jan 2014              | –   | –      | –   | –      | –                               | –    |
| Feb 2014              | 3.2   | 3.8    | 2.2   | 2.4    | –                               | –    |
| Mar 2014              | 177.1   | 181.2  | 69.8  | 75.5   | 39.4                            | 41.7 |
| Apr 2014              | 576.4   | 581.9  | 332.7   | 289.1  | 57.7                            | 49.7 |
| May 2014              | 902.1   | 915.4  | 537.7   | 484.8  | 59.6                            | 53.0 |
| Jun 2014              | 1011.9  | 1026.8 | 597.4   | 560.0  | 59.0                            | 54.5 |
| Jul 2014              | 984.5   | 998.9  | 434.6   | 342.6  | 44.1                            | 34.3 |
| Aug 2014              | 747.5   | 756.7  | 344.3   | 348.3  | 46.1                            | 46.0 |
| Aug 2013–<br>Jul 2014 | 4739.7  | 4807.3 | 2322.6  | 2089.4 | 49.0                            | 43.5 |

Table 4

Pearson linear correlation coefficients between cloudiness (C), sunshine duration (SS), relative air humidity (f), water vapour pressure (e) and mean daily solar radiation fluxes at Kaffiøyra in the period 21.07–31.08 in the years 2010–2014.

| Fluxes        | C            | SS           | f            | e           |
|---------------|--------------|--------------|--------------|-------------|
| $K\downarrow$ | <b>-0.71</b> | <b>0.79</b>  | <b>-0.32</b> | -0.14       |
| $K\uparrow$   | <b>-0.71</b> | <b>0.76</b>  | <b>-0.34</b> | -0.14       |
| $L\downarrow$ | <b>0.55</b>  | <b>-0.55</b> | <b>0.34</b>  | <b>0.47</b> |
| $L\uparrow$   | -0.09        | 0.15         | 0.01         | <b>0.52</b> |
| $K^*$         | <b>-0.70</b> | <b>0.79</b>  | <b>-0.32</b> | -0.14       |
| $L^*$         | <b>0.61</b>  | <b>-0.63</b> | <b>0.34</b>  | 0.23        |
| $Q^*$         | <b>-0.50</b> | <b>0.59</b>  | -0.19        | -0.04       |

Bold values are given at the level of significance of 0.05.

correlation ( $r = -0.70$ ), whereas longwave components of the radiation balance ( $Q^*$ ) revealed a positive correlation with cloudiness. At a higher degree of cloudiness, a large portion of  $L_{\downarrow}$  returns to the ground ( $r = 0.55$ ), therefore the longwave radiation balance was more favourable (for  $L^*$   $r = 0.61$ ).

The sunshine duration, being a measure of the amount of direct solar radiation reaching the ground, was positively correlated with the shortwave components of  $Q^*$ . Both  $K_{\downarrow}$  and  $K_{\uparrow}$  were positively dependent (with  $r = 0.79$  and  $0.76$ , respectively), and  $K^*$  was positively correlated, as well ( $r = 0.79$ ). On the other hand, the flux of  $L_{\downarrow}$  and the longwave radiation balance,  $L^*$ , revealed negative relationships ( $r = -0.55$  and  $-0.63$  respectively). With clear sky,  $L_{\downarrow}$  became noticeably lower. A higher water vapour content in the air has a negative effect on the shortwave radiation balance ( $r = -0.32$  for the relative humidity measured on 2 meters over the surface) and positive on longwave fluxes of  $L_{\uparrow}$  and  $L_{\downarrow}$  ( $r = 0.47$  and  $0.52$  for the water vapour pressure).

The solar radiation balance in the summer season at KH was significantly correlated with cloudiness ( $r = -0.50$ ). A reduction in the amount of incoming shortwave radiation,  $K_{\downarrow}$ , caused by clouds, leads to a decrease in  $Q^*$ , which indicates a dominant role of incoming solar energy in the determination of summer radiation balance.

**Surface-dependent radiation balance variability in the summer season.** — Summer months are of utmost importance for the radiation balance on Spitsbergen. That is when the amount of incoming solar radiation increases and when the surface albedo is reduced on non-glaciated land, after the snow cover melts away. However, on glaciers a high albedo is maintained throughout the year (in summer in their upper parts, covered with snow). On uncovered surfaces the albedo depends on the type of surface and vegetation.

Due to the relatively short distance between the observation sites, the key elements influencing the amount of incoming solar radiation are cloudiness and atmospheric transparency (particularly aerosol and water vapour content). On the basis of data from 2010–2014, slight differences were noted between the sites during the common period of observations, 21 July–31 August (Table 5, Fig. 4). In August, at NYA the  $K_{\downarrow}$  was  $81.8 \text{ Wm}^{-2}$  ( $297.0 \text{ MJ m}^{-2}$ ), whereas at KH it was  $83.3 \text{ Wm}^{-2}$  ( $302.1 \text{ MJ m}^{-2}$ ) and at LW2 only  $77.1 \text{ Wm}^{-2}$  ( $279.7 \text{ MJ m}^{-2}$ ).

On the other hand, the reflected  $K_{\uparrow}$  depends on the type of active surface and, in particular, on whether or not it is covered with snow. Therefore, some reflections of solar radiation occurred on tundra ground (NYA, KT) and on moraines (KH, LW1), while the snow/ice surface of the Waldemar Glacier (LW2) the amount of reflected radiation was a few times greater. In 2010–2014, in August, the mean sum of  $K_{\uparrow}$  was  $16.7 \text{ Wm}^{-2}$  ( $44.6 \text{ MJ m}^{-2}$ ) at NYA. It was similar at KH, but at LW2 it reached as much as  $56.2 \text{ Wm}^{-2}$  ( $150.5 \text{ MJ m}^{-2}$ ).

Table 5

Mean values of radiation balance fluxes at Ny-Ålesund (NYA), Kaffiøyra (KH) and Waldemar Glacier (LW) in summer seasons 2010–2014. Symbol explanations on page 62.

| Period | 21 Jul–31 Aug (MJm <sup>-2</sup> day <sup>-1</sup> ) |      |                 |                  |                  | 1–31 Aug (MJm <sup>-2</sup> ) |        |                 |                  |       |
|--------|--|------|-----------------|------------------|------------------|-------------------------------|--------|-----------------|------------------|-------|
|        | NYA  | KH   | KT <sup>1</sup> | LW1 <sup>2</sup> | LW2 <sup>3</sup> | NYA                           | KH     | KT <sup>1</sup> | LW1 <sup>2</sup> | LW2   |
| K↓     | 10.4   | 10.4 | 10.5            | 10.7             | 9.7              | 297.0                         | 302.1  | 281.1           | 324.8            | 279.7 |
| K↑     | 1.5  | 1.5  | 1.5             | 1.4              | 5.3              | 44.6                          | 44.3   | 39.0            | 44.9             | 150.5 |
| A (%)  | 15   | 15   | 14              | 13               | 55               | 15                            | 15     | 14              | 14               | 54    |
| L↑     | 30.0   | 30.7 | 31.1            | 29.9             | 29.0             | 922.4                         | 944.9  | 954.5           | 921.8            | 911.9 |
| L↓     | 26.2   | 27.3 | 28.0            | 27.3             | 27.5             | 807.9                         | 844.6  | 863.3           | 834.8            | 846.6 |
| K*     | 8.9  | 8.9  | 9.1             | 9.3              | 4.4              | 252.4                         | 257.8  | 242.1           | 279.9            | 129.2 |
| L*     | -3.8   | -3.3 | -3.1            | -2.6             | -1.5             | -114.5                        | -100.3 | -91.2           | -87.0            | -65.3 |
| Q*     | 5.1  | 5.5  | 6.0             | 6.7              | 2.9              | 138.0                         | 157.5  | 150.9           | 192.9            | 63.9  |

<sup>1</sup> – in the years 2011–2012, <sup>2</sup> – in 2010, <sup>3</sup> – in 2013 in the period 1–31 August.

This resulted from a substantial albedo, whose average value at LW2 in August was 54%, compared to just 14% at NYA and KH. Similar values were registered at KT and at LW1. In the analysed years, the albedo at LW2 varied from 91% after snowfalls to 30% after the snow melted and with a large quantity of rock material on the glacier. The shortwave radiation balance (K\*) is the most positive in the tundra areas (NYA, KT), where it reached 8 to 10 MJ m<sup>-2</sup> per day in some years (Table 5). A little lower values were recorded on the moraines (KH, LW1) and on glacial surfaces (LW2) K\* was definitely lower (about 3 to 5 MJ m<sup>-2</sup> per day).

Longwave radiation fluxes depend on the temperature of the emitting surface. In the summer season, considerable warming of the ground on Spitsbergen occurs (Araźny 2012; Araźny *et al.* 2016) and only on glaciers the temperatures remain below zero or raise to 0°C at the time of snow or ice thaw. The average upward terrestrial radiation flux (L) during the common period of 21 July–31 August was about 30 MJ m<sup>-2</sup> per day on the research area.

The downward atmospheric radiation (L↓) in the analysed period in August was 807.9 MJ m<sup>-2</sup> (NYA), 844.6 MJ m<sup>-2</sup> (KH) and 846.6 MJ m<sup>-2</sup> (LW2). The longwave radiation balance (L\*) was negative and the biggest radiative energy losses occurred in the tundra (NYA, KT) and on the moraine (KH). On glacial surfaces (LW2), the balance was least negative, which resulted from a smaller radiation emittance of the chilled surface.

The solar radiation balance, Q\*, comprises all radiation fluxes. It is positive in the summer season, when the incoming solar radiation is available 24 hours

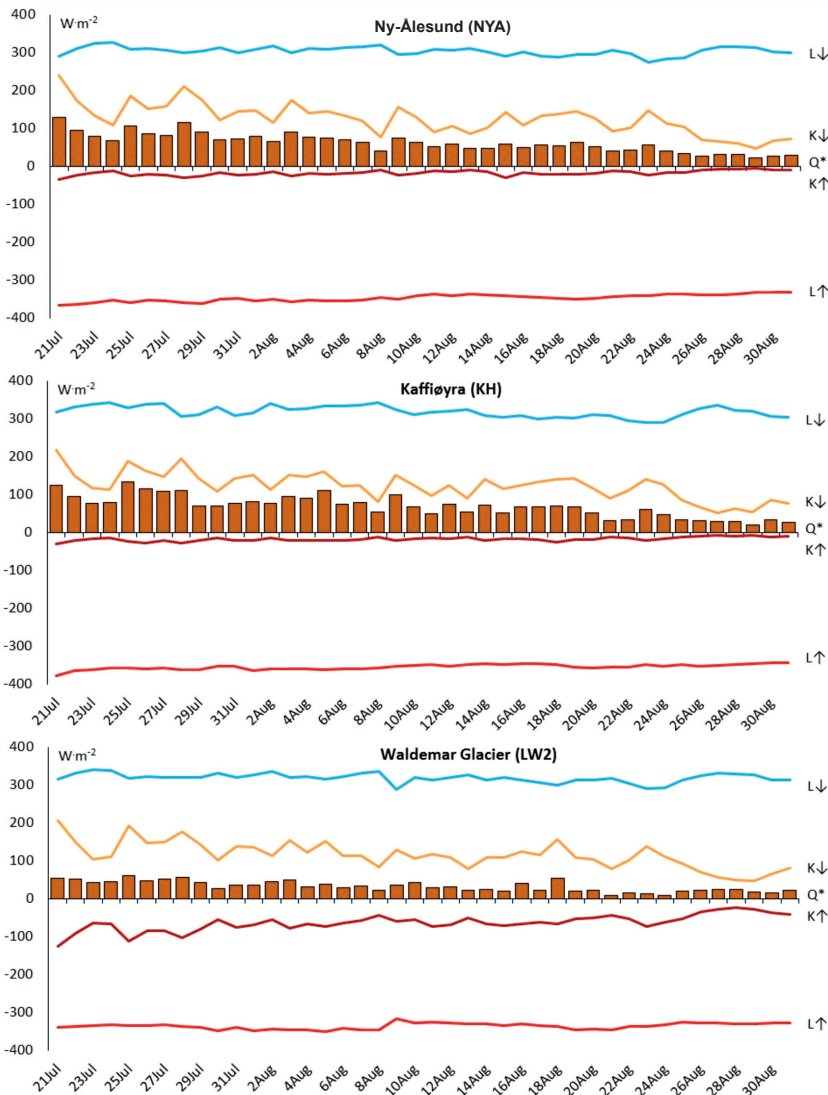


Fig. 4. Mean course of radiation balance fluxes on Ny-Ålesund, Kaffiøyra and Waldemar Glacier in the period 21 July – 31 August in the years 2010–2014. Symbol explanations on page 62.

per day. From 21 July to 31 August, the mean diurnal radiation balance reached from  $5.8 MJ m^{-2}$  at the NYA site (in 2014) to  $6.7 MJ m^{-2}$  at LW1 (in 2010). In the firn field of the Waldemar Glacier (LW2) it was substantially lower (between  $1.5 MJ m^{-2}$  in 2010 and  $4.4 MJ m^{-2}$  in 2011) – Table 5.

The monthly sums of  $Q^*$  in August were the highest at the KH site ( $156.8 MJ m^{-2}$ ) and lower at NYA ( $138.0 MJ m^{-2}$ ), but the lowest values

were obtained for LW2 (71.1 MJ m<sup>-2</sup>). There is a considerable year-on-year variability of Q\* in the firn field of the Waldemar Glacier (from 36.9 MJ m<sup>-2</sup> to 107.8 MJ m<sup>-2</sup>), which is an effect of weather changes occurring in those summer seasons. In certain years, the snow cover at the measurement site melted and the albedo of thus uncovered glacier ice is lower. In some seasons, the snow persisted throughout the season and there were frequent snowfalls, increasing the local albedo.

**Diversity of radiation balance components in diurnal course.** — The solar radiation balance Q\* reveals some diversity which is dependent on the time of day and the changing elevation of the sun. Comparing the two sites at KH (morainal surface) and at LW2 (snow/glacial surface), slight differences in the course of K↓ were found in the period from 21 July to 31 August 2010–2014 (Fig. 4). At KH, the highest mean values exceeding 220 Wm<sup>-2</sup> were recorded at midday, whereas at the time of the lower culmination of the sun these dropped to 25 Wm<sup>-2</sup>. Similar values were observed at LW2, but the maximum occurred one hour later, as the site was overshadowed and the southern horizon was obstructed by mountain ridges. Greater differences were found in the case of K↑: there was more reflected radiation at LW2 (over 130 Wm<sup>-2</sup>) than at KH (32 Wm<sup>-2</sup>). The albedo changed with the surface, revealing a distinct diurnal course with the highest values when the sun was low over the horizon (KH: from 8% to 14% and LW2: from 55% to 68% (Fig. 5). The upward terrestrial radiation (L↑) demonstrated a clear surface temperature-dependent variability. Both at KH and LW2 distinct diurnal courses of K↓ were observed, with the maximum values at afternoon hours: 371.6 Wm<sup>-2</sup> at 13:00 local time (KH), however at LW2 the highest values were recorded a few hours later: 330.4 Wm<sup>-2</sup> at 18:00. The values of L↓ were similar and did not reveal any major differences within 24 hours, reaching 329.5 Wm<sup>-2</sup> at KH and 330.4 Wm<sup>-2</sup> at LW2.

The shortwave radiation balance (K\*) was positive throughout the day, however its value on the moraine was twice as high as on the glacier, ranging from 10.4 Wm<sup>-2</sup> to 194.9 Wm<sup>-2</sup> at KH and from 6.0 Wm<sup>-2</sup> to 105.7 Wm<sup>-2</sup> at LW2. On the other hand, the longwave radiation balance (L\*) was negative throughout the day, yet smaller losses were observed on the glacier (up to -23.4 Wm<sup>-2</sup> on average) than on the moraine (up to -43.5 Wm<sup>-2</sup> on average). The total solar radiation (Q\*) in the second half of the polar summer was positive on the moraine (KH) from 3:00 to 22:00 with the maximum (152.4 Wm<sup>-2</sup>) at afternoon hours, whereas on the glacier (LW2), it was positive from 4:00 to 18:00 with the maximum reaching 82.3 Wm<sup>-2</sup> on average.

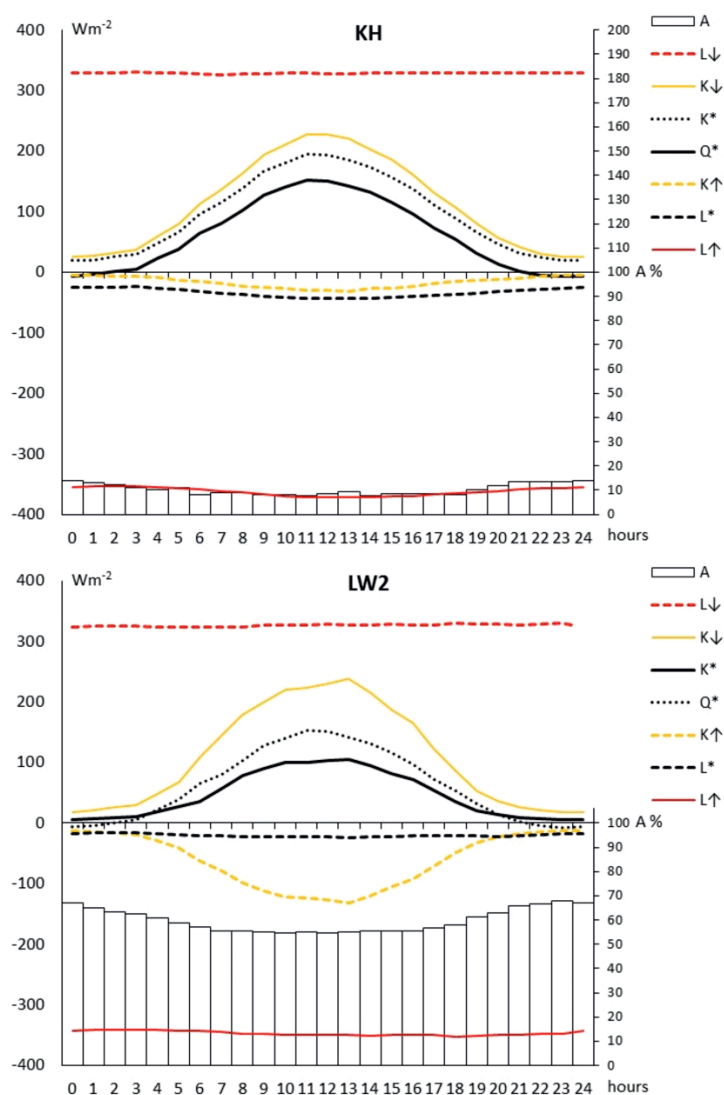


Fig. 5. Mean daily course of radiation balance fluxes and albedo at KH and LW2 stands in the period 21 July to 31 August in the years 2010–2014. Symbol explanations on page 62.

## Discussion and conclusion

The results of the measurements of the solar radiation balance components, taken at Ny-Ålesund and Kaffiøyra on NW Spitsbergen revealed a considerable local variability, dependent on the type of surface (tundra, moraine, snow and ice), as well as the exposure and shading of the site.

On NW Spitsbergen, only a small portion of solar radiation reaches the ground, mostly due to a high degree of cloudiness. A greater  $K_{\downarrow}$  was registered at the NYA site (the annual sum from August 2013 to July 2014 was  $2322.6 \text{ MJ m}^{-2}$ ), situated further to the north, than at KH ( $2089.4 \text{ MJ m}^{-2}$ ). The mean annual atmospheric transmittance of  $K_{\downarrow}$  was 49.0% at NYA and 43.5% at KH. The highest degree of transmittance at the two sites was observed in May (59.6% and 53.0%, respectively) and June (59.0% and 54.5%). The greatest influx of  $K_{\downarrow}$  occurred in June 2014:  $597.4 \text{ MJ m}^{-2}$  (NYA) and  $560.0 \text{ MJ m}^{-2}$  (KH). The annual sums were slightly lower than multi-year values determined at NYA:  $2402 \text{ MJ m}^{-2}$  for 1989–2003 (Budzik 2004) and  $2459.8 \text{ MJ m}^{-2}$  for 2008–2009 (Westermann *et al.* 2009). The albedo in the analysed year was higher as in the period 1989–2003. Therefore,  $K^*$  was lower and reached  $1011.8 \text{ MJ m}^{-2}$ , whereas in the multi-annual period its mean value was  $1177.7 \text{ MJ m}^{-2}$  (Budzik 2004). Longwave components at NYA were as follows:  $9205.2 \text{ MJ m}^{-2}$  for  $L_{\uparrow}$  and  $8190.0 \text{ MJ m}^{-2}$  for  $L_{\downarrow}$ , as compared with respective multiyear means:  $9027.2 \text{ MJ m}^{-2}$  and  $7907.0 \text{ MJ m}^{-2}$ . The value of  $L_{\uparrow}$  was found to be strongly dependent on the temperature of the ground, whereas  $L_{\downarrow}$  was correlated with the degree of cloudiness (Westermann *et al.* 2009). In the analysed year, the longwave radiation balance ( $L^*$ ) at NYA was negative:  $-1015.2 \text{ MJ m}^{-2}$  (multi-annual mean value:  $-1120.3 \text{ MJ m}^{-2}$ ). The total radiation balance ( $Q^*$ ) at the same site in 1989–2003 changed year by year from positive values ( $194 \text{ MJ m}^{-2}$ ) to negative values ( $-71 \text{ MJ m}^{-2}$ ) and its mean value was  $57.4 \text{ MJ m}^{-2}$  (Budzik 2004). In the analysed year,  $Q^*$  was  $-3.4 \text{ MJ m}^{-2}$ .

The observations carried out in 2001–2010 at the Kongsvegen Glacier near Ny-Ålesund (Karner *et al.* 2013) indicated that at 537 m a.s.l. more  $K_{\downarrow}$  ( $2942.3 \text{ MJ m}^{-2}$ ) reaches the ground than at the NYA site. This resulted from a higher content of water vapour and aerosol in the lower layer of the atmosphere. However, due to the high albedo of snow-ice surface  $K^*$  is just  $722.2 \text{ MJ m}^{-2}$ . Longwave components of radiation balance were lower ( $L_{\uparrow}$   $8527.2 \text{ MJ m}^{-2}$  and  $L_{\downarrow}$   $7770.5 \text{ MJ m}^{-2}$ ), but the glacier area lost less energy:  $L^* = -756.9 \text{ MJ m}^{-2}$ . The radiation balance on that glacier was negative:  $-34.7 \text{ MJ m}^{-2}$ .

The radiation balance  $Q^*$  and its individual components revealed a considerable spatial variability on Spitsbergen. The decisive factor was, however, not the latitude but the local weather, exposure and obstruction of the horizon (Kryza *et al.* 2010), and – in particular – the type of surface. An analysis of meteorological determinants of the components of  $Q^*$  at KH in the summer seasons of 2010–2014 confirmed a negative effect of cloudiness on the shortwave components. As cloudiness increases the amount of incoming solar radiation  $K_{\downarrow}$  is reduced, and so are direct solar radiation,  $K_{\uparrow}$  and  $K^*$ . On the other hand, both  $L_{\downarrow}$  and  $L^*$  increase. During the polar day  $Q^*$  at KH is negatively correlated with the cloud amount. On bright days the individual components of  $Q^*$  become different between the various surfaces, whereas on cloudy days these differences



are smaller (Bintanja 1995; Kejna 2012). Nevertheless, in the analysed years the so-called radiation paradox, typical of polar areas in both hemispheres, where  $Q^*$  takes higher values in the presence of thick clouds (Bintanja and van den Broeke 1996a, b), did not occur at KH. The radiation paradox is an effect of multiple reflections of  $K_{\downarrow}$  from the surface and the cloud base (Westermann *et al.* 2009). An analysis of the relationships between individual fluxes with the sunshine duration revealed positive correlations with  $K_{\downarrow}$  and  $K_{\uparrow}$ , but negative ones with  $L_{\downarrow}$  and  $L^*$ . Despite substantial radiation losses connected with  $L_{\uparrow}$  (a surface undergoes considerable warming at extensive sunshine duration and there is greater emittance of longwave radiation),  $Q^*$  revealed a positive correlation.

The radiation balance  $Q^*$  undergoes variations in a diurnal course, depending on the elevation of the sun. An analysis of typically polar surfaces confirmed an essential role of albedo for the shaping of  $K^*$ , which was twice lower on glacial surfaces and reached the highest values at the time of a maximum influx of  $K_{\downarrow}$ . On the other hand,  $L^*$  was negative throughout the day and revealed a diurnal variability, depending on the temperature of the surface. Greater losses of heat ( $L^*$ ) were observed on the moraine than on snow- or ice-covered surfaces, whose temperature did not exceed the ice melting point. The most evident differences between the sites were observed in the afternoon, when non-glaciated surfaces become considerably warmed up and thus  $L_{\uparrow}$  increases. On snow and ice covered surfaces  $L^*$  reaches the highest values at 18:00, similarly as it is in other polar regions, *e.g.* in the Antarctica (Bintanja 1995). In the analysed period,  $Q^*$  during the polar day was positive, however when the sun was lower over the horizon, from 3:00 to 22:00 at KH and from 4:00 to 18:00 at LW2, energy losses prevailed.

The values of individual components of  $Q^*$  obtained for NW Spitsbergen are consistent with measurements taken in other areas of the island (Table 6). For the comparable month of August, on non-glaciated surfaces  $K_{\downarrow}$  ranged from 234.7 MJ m<sup>-2</sup> at the forefield of the Werenskiold Glacier to 306.7 MJ m<sup>-2</sup> at Petuniabukta.

On glaciated surfaces at the Waldemar Glacier, the mean  $K_{\downarrow}$  was 279.7 MJ m<sup>-2</sup>, whereas in the area of Southern Spitsbergen on the Hans Glacier it was 363 MJ m<sup>-2</sup> in 2009, and 361.5 MJ m<sup>-2</sup> on the Werenskiold Glacier in 1957–1960. The solar radiation balance is significantly affected by the albedo of the active surface, which in the case of the tundra ranges from 8.5% at Calypso (Bellsund) to 16% at Hornsund, and on snow-covered and glaciated surfaces reaches 54% (Waldemar Glacier) and 58% (Hans Glacier), although it depends on the state of the surface. The longwave radiation balance was negative, smaller on glaciers (*e.g.* -53 MJ m<sup>-2</sup> on the Waldemar Glacier and -56 MJ m<sup>-2</sup> on the Hans Glacier) than on warmer surfaces of the tundra or moraines (*e.g.* -114.5 MJ m<sup>-2</sup> at NYA). A higher temperature of the surface results in an increase in  $L_{\uparrow}$ . In August,  $Q^*$  is positive on Spitsbergen and reaches

Table 6

Values of balance radiation fluxes in August on Spitsbergen.

| Area                           | Years                  | K↓                | K↑                | A      | L↑                | L↓                | K*                | L*                | Q*                |
|--------------------------------|------------------------|-------------------|-------------------|--------|-------------------|-------------------|-------------------|-------------------|-------------------|
|                                |                        | MJm <sup>-2</sup> | MJm <sup>-2</sup> | %      | MJm <sup>-2</sup> | MJm <sup>-2</sup> | MJm <sup>-2</sup> | MJm <sup>-2</sup> | MJm <sup>-2</sup> |
| Ny-Ålesund                     | 1989–2003 <sup>1</sup> | 267.6             |                   |        |                   |                   | 224.6             | -104.2            | 120.4             |
|                                | 2008 <sup>2</sup>      | 269.7             | 41.2              | 15     | 909.6             | 810.6             | 228.5             | -99.0             | 129.5             |
|                                | 2010–2014              | 297.0             | 44.6              | 15     | 922.4             | 807.9             | 252.5             | -114.5            | 138.0             |
| Kaffiøyra region               | KH<br>(2010–2014)      | 302.1             | 44.3              | 15     | 944.9             | 844.5             | 257.0             | -100.4            | 156.8             |
|                                | LW2<br>(2010–2014)     | 279.7             | 150.5             | 54     | 911.9             | 858.7             | 128.2             | -53.2             | 71.1              |
| Hornsund                       | 1978–2006 <sup>3</sup> | 300.3             |                   |        |                   |                   |                   |                   |                   |
|                                | 2008 <sup>2</sup>      | 275.6             | 43.7              | 16     | 911.6             | 810.8             | 231.9             | -100.9            | 131               |
| Werenskiold<br>Glacier-moraine | 1970–1973 <sup>3</sup> | 234.7             |                   |        |                   |                   |                   |                   |                   |
| Werenskiold<br>Glacier-ice     | 1957–1960 <sup>3</sup> | 361.5             |                   |        |                   |                   |                   |                   |                   |
| Hans Glacier                   | 2008 <sup>2</sup>      | 363               | 209               | 58     | 800               | 856               | 154               | -56               | 98                |
| Calypso (Bellsund)             | 2006–2008 <sup>4</sup> | 272.6             |                   | 8.5–21 |                   |                   |                   |                   |                   |
| Petuniabukta                   | 2008 <sup>5</sup>      | 289.3             |                   | 14     |                   |                   |                   |                   |                   |
|                                | 2009 <sup>5</sup>      | 306.7             |                   | 14     |                   |                   |                   |                   |                   |

References: 1 – Budzik 2004, 2 – Budzik *et al.* 2009, 3 – Marsz and Styszyńska 2007, 4 – Gluza 2010 (personal information), 5 – Láska *et al.* 2012  
 Symbol explanations on page 62.

its maximum values in non-glaciated areas: 156.8 MJ m<sup>-2</sup> (KH), 138.0 MJ m<sup>-2</sup> (NYA) and 131 MJ m<sup>-2</sup> (Hornsund). A more negative balance was observed on the glaciers: 71.1 MJ m<sup>-2</sup> (Waldemar Glacier) and 98 MJ m<sup>-2</sup> (Hans Glacier).

Energy incomes or losses, resulting from the solar radiation balance, affect the functioning of the environment. In the Arctic, an increase in radiation balance is observed, particularly connected with changes in its longwave components (Wang and Dickinson 2013; Marturilli 2014). In polar conditions, individual fluxes of Q\* influence the temperature of the ground, its thawing depth and the thickness of permafrost (Werstermann 2009; Sobota and Nowak 2014; Arażny *et al.* 2016). Snow cover melts more quickly, the rate of ablation increases and a considerable glacial recession occurs with a negative mass balance of glaciers (cf. Sobota and Lankauf 2010; Karner *et al.* 2013).

**Acknowledgements.** — This study was developed within the framework of a research project “Contemporary and historical changes in the Svalbard climate and topoclimates” (NCN No. DEC-2011/03/B/ST10/05007. The authors wish to thank the participants of polar expeditions to Kaffiøyra: Edward Łaszyca, Tomasz Strzyżewski and Patrycja Ulandowska-Monarcha for their support in actinometrical observations. Special thanks go to journal referees Krystyna Bryś and Kajsa Maria Parding for their comments that have helped to improve the manuscript.

## References

- ARAŻNY A. 2012. Ground temperature. *In*: R. Przybylak, A. Arażny and M. Kejna (eds.) *Topoclimatic diversity in Forlandsundet region (NW Spitsbergen) in global warming conditions*. Oficyna Wydawnicza “Turpress”, Toruń: 77–88.
- ARAŻNY A., PRZYBYŁAK R. and KEJNA M. 2016. Ground temperature changes on the Kaffiøyra Plain (Spitsbergen) in the summer seasons, 1975–2014. *Polish Polar Research* 37: 1–21.
- ARNOLD N. and REES G. 2009. Effects of digital elevation model spatial resolution on distributed calculations of solar radiation loading on a High Arctic glacier. *Journal of Glaciology* 55: 194: 973–984.
- BINTANJA R. 1995. The local energy balance of the Ecology Glacier, King George Island, Antarctica: Measurements and modelling. *Antarctic Science* 7: 315–325.
- BINTANJA R. and VAN DEN BROEKE M.R. 1996a. The influence of clouds on the radiation budget of ice and snow surfaces in Antarctica and Greenland in summer. *International Journal of Climatology* 16: 1281–1296.
- BINTANJA R. and VAN DEN BROEKE M.R. 1996b. The surface energy balance of Antarctic snow and blue ice. *Journal of Applied Meteorology* 34: 902–926.
- BUDZIK T. 2003. The structure of solar balance radiation in the area of the Aavatsmark glacier held from April 13 to May 4, 2002. *Problemy Klimatologii Polarnej* 13: 151–160 (in Polish).
- BUDZIK T. 2004. The structure of solar balance radiation in Ny-Ålesund (Spitsbergen) in the years 1989 and 2003. *Problemy Klimatologii Polarnej* 14: 189–197 (in Polish).
- BUDZIK T., SIKORA S. and ARAŻNY A. 2009. Annual radiation balance course of the active surface in Hornsund (May 2008 – April 2009). *Problemy Klimatologii Polarnej* 19: 233–246 (in Polish).

- CAPUTA Z., GRABIEC M. and LULEK A. 2002. The structure of the radiation balance on Aavatsmarka Glacier from 11 to 30 April 2001. *In: A. Kostrzewski and G. Rachlewicz (eds.) Funkcjonowanie i monitoring geosystemów obszarów polarnych*, Poznań: 96–103 (in Polish).
- CURRY J.A., ROSSOW W.B., RANDALL D. and SCHRAMM J.L. 1996. Overview of Arctic cloud and radiation characteristics. *Journal of Climate* 9: 1731–1764.
- DUYNKERKE P.G. and VAN DEN BROEKE M.R. 1994. Surface energy balance and katabatic flow over glacier and tundra during GIMEX-91. *Global Planete Change* 9: 17–28.
- EASTMAN R. and WARREN S.G. 2010. Interannual variations of Arctic cloud types in relation to sea ice. *Journal of Climate* 23: 4216–4232.
- ETZELMÜLLER B., SCHULER T.V., ISAKSEN K., CHRISTIANSEN H.H., FARBROT H. and BENESTAD R. 2011. Modeling the temperature evolution of Svalbard permafrost during the 20th and 21st century. *The Cryosphere* 5: 67–79.
- GLUZA A. and SIWEK K. 2005. Albedo differentiation of Calypsostranda (West Spitsbergen) in summer 2001. *Problemy Klimatologii Polarnej* 15: 113–117 (in Polish).
- GŁOWICKI B. 1985. Radiation conditions in the Hornsund area (Spitsbergen). *Polish Polar Research* 6: 301–318.
- HARTMANN D.L. 1994. *Global Physical climatology*. Academic Press, New York: 408 pp.
- HISDAL V. 1986. Spectral distribution of global and diffuse solar radiation in Ny-Ålesund. Spitsbergen. *Polar Research* 5: 1–27.
- HISDAL V., FINNEKÅSA Ø. and VINJE T. 1992. Radiation measurements in Ny-Ålesund. Spitsbergen 1981–1987. *Meddelelser* 118, Norsk Polarinstitut, Oslo. 380 pp.
- ISAKSEN K., NORDLI Ø., FØRLAND E.J., ŁUPIKASZA E., EASTWOOD S. and NIEDŹWIEDŹ T. 2016. Recent warming on Spitsbergen—Influence of atmospheric circulation and sea ice cover, *Journal of Geophysical Research Atmospheres* 121: 11913–11931.
- KARNER F., OBLEITNER F., KRISMER T., KOHLER J. and GREUILL W. 2013. A decade of energy and mass balance investigations on the glacier Kongsvegen, Svalbard. *Journal of Geophysical Research: Atmospheres* 118: 3986–4000.
- KEJNA M. 2000. Albedo of the Waldemar glacier surface (Spitsbergen) in summer season 1999. *In: Polish Polar Studies, 27th International Polar Symposium, Toruń*: 181–190.
- KEJNA M., PRZYBYŁAK R. and ARAŻNY A. 2011. Spatial differentiation of radiation balance in the Kaffiøyra region (Svalbard, Arctic) in the summer season 2010. *Problemy Klimatologii Polarnej* 21: 173–186.
- KEJNA M. 2012. Radiation conditions. *In: R. Przybylak, A. Arażny, M. Kejna (eds.) Topoclimatic diversity in Forlandsundet region (NW Spitsbergen) in global warming conditions*. Oficyna Wydawnicza “Turpress”, Toruń: 53–76.
- KEJNA M., USCKA-KOWALKOWSKA J., ARAŻNY A., KUNZ M., MASZEWSKI R. and PRZYBYŁAK R. 2014. Spatial differentiation of global solar radiation in Toruń and its suburban area (central Poland) in 2012. *Bulletin of Geography - Physical Geography Series* 7: 27–56.
- KRYZA M., SZYMANOWSKI M. and MIGAŁA K. 2010. Spatial information on total solar radiation: Application and evaluation of the sun model for the Wedel Jarlsberg Land. Svalbard. *Polish Polar Research* 31: 17–32.
- KOSIBA A. 1960. Some of results of glaciological investigations in SW-Spitsbergen. *Zeszyty Naukowe Uniwersytetu Wrocławskiego* B4: 3–30.
- KUPFER H., HERBER A. and KÖNIG-LANGLO G. 2006. *Radiation measurements and synoptic observations at Ny-Ålesund. Svalbard*. Reports on Polar and Marine Research, Alfred Wegener Institute for Polar and Marine Research, Bremerhaven: 115 pp.
- LÁSKA K., WITOSZOVÁ D. and PROŠEK P. 2012. Weather patterns of the coastal zone of Petuniabukta, central Spitsbergen in the period 2008–2010. *Polish Polar Research* 33: 297–318.

- MARSZ A. and STYSZYŃSKA A. 2007. *Climate of the region of Polish Polar Station in Hornsund*. Wydawnictwo Akademii Morskiej, Gdynia: 376 pp. (in Polish).
- MATURILLI M., HERBER A. and KÖNIG-LANGLO G. 2013. Climatology and time series of surface meteorology in Ny-Ålesund, Svalbard. *Earth System Science Data* 5: 155–163.
- MATURILLI M., HERBER A. and KÖNIG-LANGLO G. 2015. Surface radiation climatology for Ny-Ålesund, Svalbard (78.9° N). basic observations for trend detection. *Theoretical and Applied Climatology* 120: 331–339.
- NARDINO M. and GEORGIADIS T. 2003. Cloud type and cloud cover effects on the surface radiative balance at several polar sites. *Theoretical and Applied Climatology* 74: 203–215.
- NORDLI Ø., PRZYBYŁAK R., OGILVIE A.E.J. and ISAKSEN K. 2014. Long-term temperature trends and variability on Spitsbergen: the extended Svalbard Airport temperature series, 1898–2012. *Polar Research* 33: 21349.
- NUTH C., KOHLER J., KÖNIG M., VON DESCHWANDEN A., HAGEN J.O., KÄÄB A., MOHOLDT G. and PETERSSON R. 2013. Decadal changes from a multi-temporal glacier inventory of Svalbard. *The Cryosphere* 7: 1603–1621.
- OKE T.R. 1987. *Boundary layer climates*. Routledge, London New York: 435 pp.
- ØRBAEK J.B., HISDAL V. and SVAASAND L.E. 1999. Radiation climate variability in Svalbard: surface and satellite observations. *Polar Research* 18: 127–134.
- PROŠEK P. and BRÁZDIL R. 1994. Energy balance of the tundra at the Spitsbergen Island (Svalbard) in the summer seasons of 1988 and 1990. *Scripta Facultatis Scientiarum Naturalium Universitatis Masarykianae Brunensis* 24 (Geography): 43–60.
- PRZYBYŁAK R. 2016. *The Climate of the Arctic*. Atmospheric and Oceanographic Sciences Library 52, Springer International Publishing Switzerland: 287 pp.
- PRZYBYŁAK R. and ARAŻNY A. 2006. Climatic conditions of the north-western part of Oscar II Land (Spitsbergen) in the period between 1975 and 2000. *Polish Polar Research* 27: 133–152.
- PRZYBYŁAK R., ARAŻNY A. and KEJNA M. (eds) 2012. *Topoclimatic diversity in Forlandsundet region (NW Spitsbergen) in global warming conditions*. Oficyna Wydawnicza “Turpress”, Toruń: 174 pp.
- SCREEN J.A. and SIMMONDS I. 2010. The central role of diminishing sea ice in recent Arctic temperature amplification. *Nature* 464: 1334–1337.
- SERREZE M.C. and BARRY R.G. 2011. Processes and impacts of Arctic amplification: A research synthesis. *Global and Planetary Change* 77: 85–96.
- SHUPE M.D. and INTRIERI J. 2004. Cloud radiative forcing of the Arctic surface: the influence of cloud properties, surface albedo, and solar zenith angle. *Journal of Climate* 17: 616–628.
- SOBOTA I. 2013. *Contemporary changes of the cryosphere of north-western Spitsbergen based on the example of the Kaffiøyra region*. Wydawnictwo Naukowe UMK: 459 pp. (in Polish).
- SOBOTA I. and LANKAUF K.R. 2010. Recession of Kaffiøyra region glaciers, Oscar II Land, Svalbard. *Bulletin of Geography – Physical Geography Series* 3: 27–45.
- SOBOTA I. and NOWAK M. 2014. Changes in the dynamics and thermal regime of the permafrost and active layer of the High Arctic coastal area in North-West Spitsbergen, Svalbard. *Geografiska Annaler A* 96: 227–240.
- STYSZYŃSKA A. 1997. Valuation of the monthly sum of the total sun radiation in Hornsund (SW Spitsbergen). In: J. Repelewska-Pękalowa and K. Pękala (eds.) *Spitsbergen Geographical Expeditions of M. Curie-Skłodowska University*. UMCS Lublin: 163–172.
- VINJE T. 1974–1982. *Radiation conditions in Spitsbergen*. Norsk Polarinstitutt Årbok, Norsk Polarinstitutt, Tromsø.
- WANG K. and DICKINSON R.E. 2013. Global atmospheric downward longwave radiation at the surface from ground-based observations, satellite retrievals, and reanalyses. *Reviews of Geophysics* 51: 150–185.

- WESTERMANN S., LUERS J., LANGER M., PIEL K. and BOIKE J. 2009. The annual surface energy budget of a high-arctic permafrost site on Svalbard, Norway. *The Cryosphere* 3: 245–263.
- WÓJCIK G. 1989. The transparency of the atmosphere and the intensity of direct solar radiation in the Arctic and Antarctic. *XVI Sympozjum Polarne*, Toruń. 19–20 września 1989 r.: 149–151 (in Polish).
- WÓJCIK G. and MARCINIAK K. 1993. The daily course of direct solar radiation in the summer on Spitsbergen. In: *Działalność naukowa Profesora Władysława Gorczyńskiego i jej kontynuacja*. Sympozjum w Uniwersytecie Mikołaja Kopernika. Toruń, Streszczenia referatów. 121–123 (in Polish).
- WÓJCIK G. and MARCINIAK K. 2002. The transparency of the atmosphere and the intensity of direct solar radiation on Kaffiöyra Plain (NW Spitsbergen) in summer 1979. *Problemy Klimatologii Polarnej* 8: 105–110 (in Polish).
- ZYGMUNTOWSKA M., MAURITSEN T., QUAAS J. and KALESCHKE L. 2012. Arctic clouds and surface radiation – a critical comparison of satellite retrievals and the ERA-interim reanalysis. *Atmospheric Chemistry and Physics* 12: 6667–6677.

Received 30 June 2016

Accepted 22 December 2016